AM-FM TEXTURE SEGMENTATION IN ELECTRON MICROSCOPIC MUSCLE IMAGING

Marios Pattichis, Constantinos Pattichis†, Maria Avraam†, Alan Bovik‡, and Kyriakos Kyriakou+*

*Department of Electrical Engineering and Computer Science
Washington State University, Pullman, WA 99164-2752
e-mail: pattichi@eecs.wsu.edu

†Department of Computer Science, University of Cyprus, Nicosia, Cyprus
e-mail: pattichi@turing.cs.ucy.ac.cy

‡Laboratory for Vision Systems, University of Texas, Austin, TX 78712-1084
e-mail: bovik@vision.ece.utexas.edu

+Department of Electron Microscopy,
The Cyprus Institute of Neurology and Genetics, Nicosia, Cyprus
e-mail: Kyriacos@mdrtc.cing.ac.cy

ABSTRACT

We segment the structural units of electron microscope muscle images using a novel AM-FM image representation. This novel AM-FM approach is shown to be effective in describing sarcomeres and mitochondrial regions of the electron microscope muscle images.

1. INTRODUCTION

Accurate diagnosis of some neuromuscular disorders requires examination of muscle biopsies with the electron microscope. Ultrastructural examination is often essential for confirming the diagnosis of metabolic myopathies and in particular those myopathies that are caused by mitochondrial abnormalities. Such abnormalities cause the accumulation of mitochondrial aggregates which disturb the very regular anatomic pattern exhibited by normal muscle fibres characterized by the repetitive arrangement of functional units, called sarcomeres.

In some patients, suspected of suffering from mitochondrial abnormalities, the mitochondrial aggregates are not as pronounced, making diagnosis difficult. In order to overcome this difficulty, a novel AM-FM segmentation method has been developed for electron microscopic muscle images. The main objective is to train the system on recognizing abnormalities that disturb the regular sarcomere structure of muscle fibres using known "typical" diagnostic cases. The ultimate objective will be to test the ability of the system to recognize "pathological abnormalities" in borderline cases in order to supplement the diagnostic ability of human experts.

2. METHOD

Ideally, sarcomeres are perfectly aligned, with sarcomeres repeating regularly both vertically and horizontally. Hence, the two dimensional Fourier series would be an appropriate representation for this ideal case:

$$I_{ideal}(x_1, x_2) = \sum_{n,m} A_{n,m} \cos(nx_1 + mx_2) \qquad (1)$$

In general images, (eg: Figures 1(*a*) and 1(*b*)), we can still model the sarcomere regions as ideal regions that have undergone local deformations. We model this deformation by a coordinate transformation from the ideal image coordinates of $x_1 - x_2$ to the deformed image coordinates $\phi_1(x_1, x_2) - \phi_2(x_1, x_2)$. We express a regular sarcomere image as the coordinate-transformed version of an ideal image [3]:

$$\begin{aligned} I_{sar}(x_1, x_2) &= I_{ideal}(\phi_1(x_1, x_2), \phi_2(x_1, x_2)) \\ &= \sum_{n,m} \cos\Big[n\phi_1(x_1, x_2) + m\phi_2(x_1, x_2) \Big] \end{aligned}$$

In addition to variations in the arrangement of the sarcomeres, we need to account for the presense of mitochondria (appearing as small dark regions). We use amplitude functions a_{sar} supported over the sarcomere regions, and a_{mit} supported over the mitochondrial regions to differentiate between the two image regions (set $\mathbf{x} = (x_1, x_2)$):

$$\begin{aligned} I(\mathbf{x}) &= a_{sar}(\mathbf{x}) \sum_{n,m} a_{n,m} \cos\Big[n\phi_1(\mathbf{x}) + m\phi_2(\mathbf{x}) \Big] \\ &\quad + a_{mit}(\mathbf{x}) \sum_{n,m} b_{n,m} \cos\Big[n\psi_1(\mathbf{x}) + m\psi_2(\mathbf{x}) \Big] \end{aligned}$$

To segment the image into sarcomeres and mitochondria structural units, we bandpass-filtered the image to extract the fundamental harmonics of the AM-FM expansions. We leave the details on how to compute these fundamental AM-FM harmonics for Section 3.

Once the fundamental AM-FM components have been determined, we use the local amplitude $a(\cdot)$ and/or the local instantaneous frequency magnitude ($\| \nabla\phi_i(\cdot) \|$ or $\| \nabla\psi_{i,1}(\cdot) \|$), to isolate the mitochondrial regions from the sarcomere regions. We

0-7803-5041-3/99 $10.00 © 1999 IEEE

expect the range of values for these two AM-FM parameters to be different for the sarcomere and the mitochondrial regions. This observation will be the basis of our segmentation algorithm.

3. IMPLEMENTATION

In this Section, we discuss how to use the dominant component analysis algorithm to estimate the fundamental AM-FM components, and then apply simple thresholding to segment the image.

We must first isolate the fundamental AM-FM components. We prefilter the image using an ideal, circularly symmetric, low-pass filter with a circular radius cutoff at 0.15 cycles per image length. The cutoff frequency allows AM-FM harmonics with an instantaneous wavlength of about 7 pixels and was empirically determined to be sufficient. Next, to estimate the AM-FM harmonics, we use the dominant component analysis (see [2], [1] for details). In the dominant component analysis algorithm, a bank of Gabor channels is applied to the image, and the channel with the maximum energy is selected for estimating the AM-FM parameters. If we let $t_m(\cdot)$ denote the channel output at the mth channel with frequency magnitude response $G_m(\cdot)$, then the AM-FM parameters are given by [2]:

$$\nabla\Phi(\mathbf{x}) \approx \mathrm{Re}\left[\frac{\nabla t_m(\mathbf{x})}{j t_m(\mathbf{x})}\right],$$

$$\Phi(\mathbf{x}) \approx \arctan\left\{\frac{\mathrm{Im}[t_m(\mathbf{x})]}{\mathrm{Re}[t_m(\mathbf{x})]}\right\}, \quad a(\mathbf{x}) \approx \left|\frac{t_m(\mathbf{x})}{G_m[\nabla\theta\mathbf{x}]}\right|$$

For our purposes, we are only interested in the amplitude $a(\cdot)$ and the instantaneous frequency magnitude $\| \nabla\phi(\cdot) \|$. To isolate the structural units of the muscle, we select thresholds for $a(\cdot)$ and $\| \nabla\phi(\cdot) \|$ using the histogram of the distribution of their values (see Figures 1 (c)-(f)). For the instantaneous frequency magnitude, we threshold between the low peaks of the histogram, while for the amplitude, we threshold at a level that appears to be at the right end of the main distribution (see the caption in Figure 2 for details).

4. RESULTS

We present the segmentation results in Figures 2 $(a) - (h)$. We first explain briefly how the values of the amplitude and the instantaneous frequency can be associated with the local structure variations of the electron micrographs. We then comment on the segmented images.

We first explain (briefly) what the AM-FM parameters are measuring. For the amplitude, we note that it describes the bounds in the local intensity variations. For example, when the local image intensity is alternating between nearly white (maximum intensity) and nearly black (minimum intensity) values, then the local amplitude is indeed large. For the instantaneous frequency magnitude, we note that it is inversely proportional to the instantaneous wavelength, that is the period of the locally repeating pattern. For example, when the repeating pattern is thin, the instantaneous wavelength is small and the instantaneous frequency magnitude is large. Since we are estimating the fundamental AM-FM components, we also expect that the segmented images will be made of regions that are as thick as the fundamental wavelength.

The sarcomeres are separated by sharp dark and white regions. Thus, between any two sarcomeres, there is large variation above and below the "local mean" image intensity, and this is described by large fundamental amplitude components for the regions between the units. Similar comments apply for the mitochondrial regions. The dark mitochondria on a white background yield very large amplitude components. Thus, it is difficult to differentiate between sarcomere boundaries and mitochondrial regions, if we only use the range of amplitude values for this purpose.

Clearly, the white and dark stripes at the boundaries of the sarcomere units are thin as compared to the size of the units. Thus, they are characterized by large instantaneous frequency magnitude $\| \nabla\phi_1(\cdot) \|$. This observation is clearly demonstrated in the resulting images in Figures 2(c), (e), (g), and also in 2(d), (f), (h).

For the normal case, overall, the boundaries of the sarcomeres have been successfully detected (see Figures 2 (a) and (e)). Furthermore, the mid-region of the sarcomeres which correspond to the I bands are also successfully detected as shown in Figure 2 (g). The rest of the sarcomeres have also been detected (as shown in Figure 2 (c)). It is evident that in these images a regular repetitive pattern is displayed which closely approximates the normal fibre structure of physiological muscle fibres.

Next, we comment om the results for the case suspected as having mitochondrial abnormalities. A definite diagnosis of mitochondrial myopathy could not be made so this was considered as borderline case. The amplitude segmented image (of Figure 2 (b)) shows that the proposed system has the potential to identify the abnormal regions. Normal regions are also included in Figure 2 (b), indicating that the system should be further enhanced in order to enable it to cope with difficult cases such as the example presented. The instantaneous frequency magnitude results of Figures 2 (d), (f) and (h) were less impressive than the corresponding images for the normal case. Nevertheless, the amplitude results of Figure 2 (b) are very promising, and it can be seen that the instantaneous frequency magnitude results can be combined with the amplitude results to improve performance (as for example by removing the sarcomeres detected in Figures 2(f) and 2(h) from the mixed sarcomere-mitochondrial regions of Figure 2(b)).

5. CONCLUDING REMARKS

Our findings although preliminary suggest that the proposed system can identify normal repetitive structure, with a good degree of accuracy. Furthermore the system is capable of detecting abnormal regions which disturb the regular pattern, such as those present in muscle pathology. More work is currently being carried out in order to make the system recognition more sensitive and impose its specificity. The wider applicapility of such systems will also enhance our ability to quantify changes that affect the cellular ultrastructure.

6. REFERENCES

[1] A. C. Bovik, N. Gopal, T. Emmoth, and A. Restrepo. Localized measurement of emergent image frequencies by Gabor wavelets. *IEEE Trans. on Information Theory*, 38(2):691–712, March 1992. Special Issue on Wavelet Transforms and Multiresolution Signal Analysis.

[2] J. P. Havlicek. *AM-FM Image Models*. PhD thesis, The University of Texas at Austin, 1996.

[3] M. S. Pattichis. *AM-FM Transforms with Applications*. PhD thesis, The University of Texas at Austin, 1998.

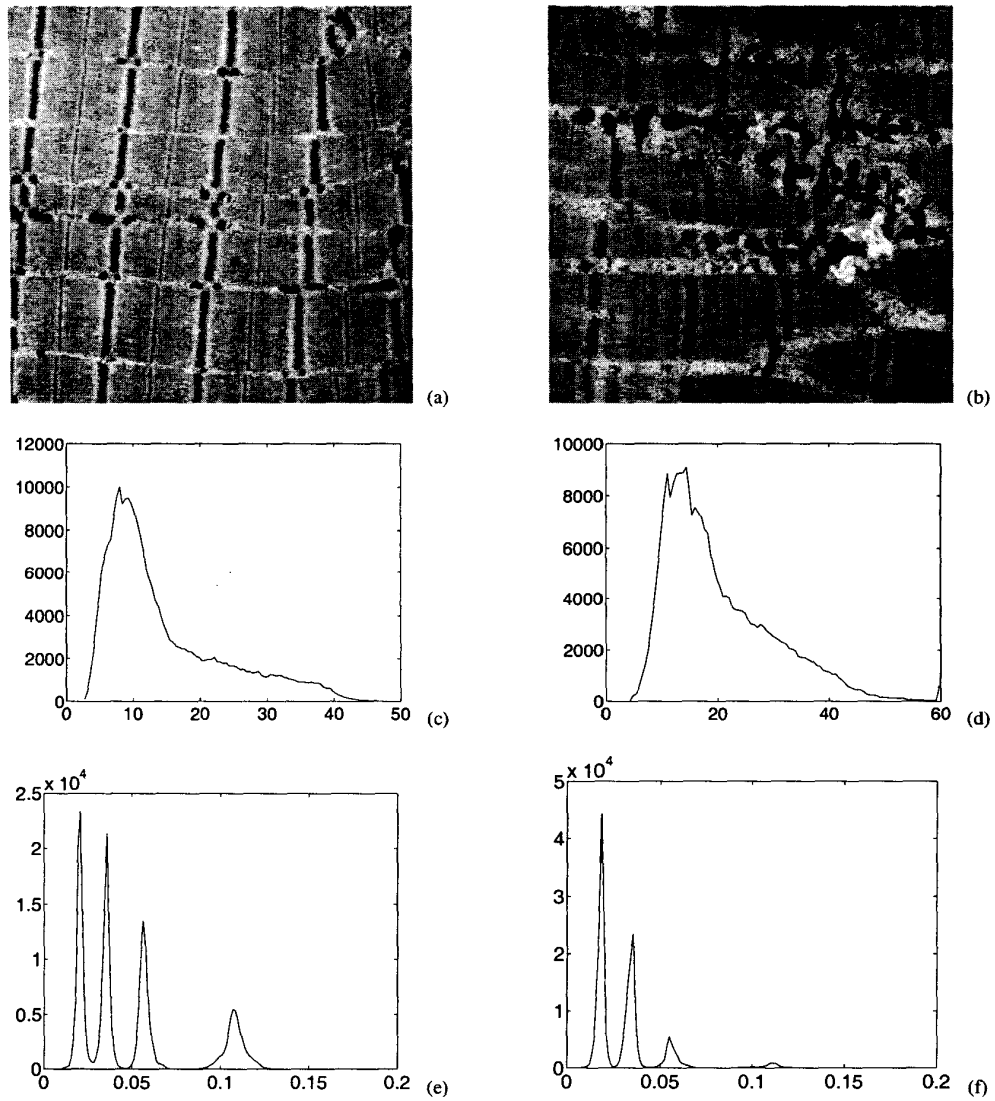

Figure 1: AM-FM analysis results I of II. In (a), we show a normal, electron microscopy image. In (b), we show a pathological case. In (c) and (d) we show the histograms of the amplitude $a(\cdot)$ distribution for all local AM-FM components. Similarly, in (e) and (f), we show the histograms of the instantaneous frequency magnitude (note that in (f) the frequencies must be multiplied by 1000 and the units are cycles per image length).

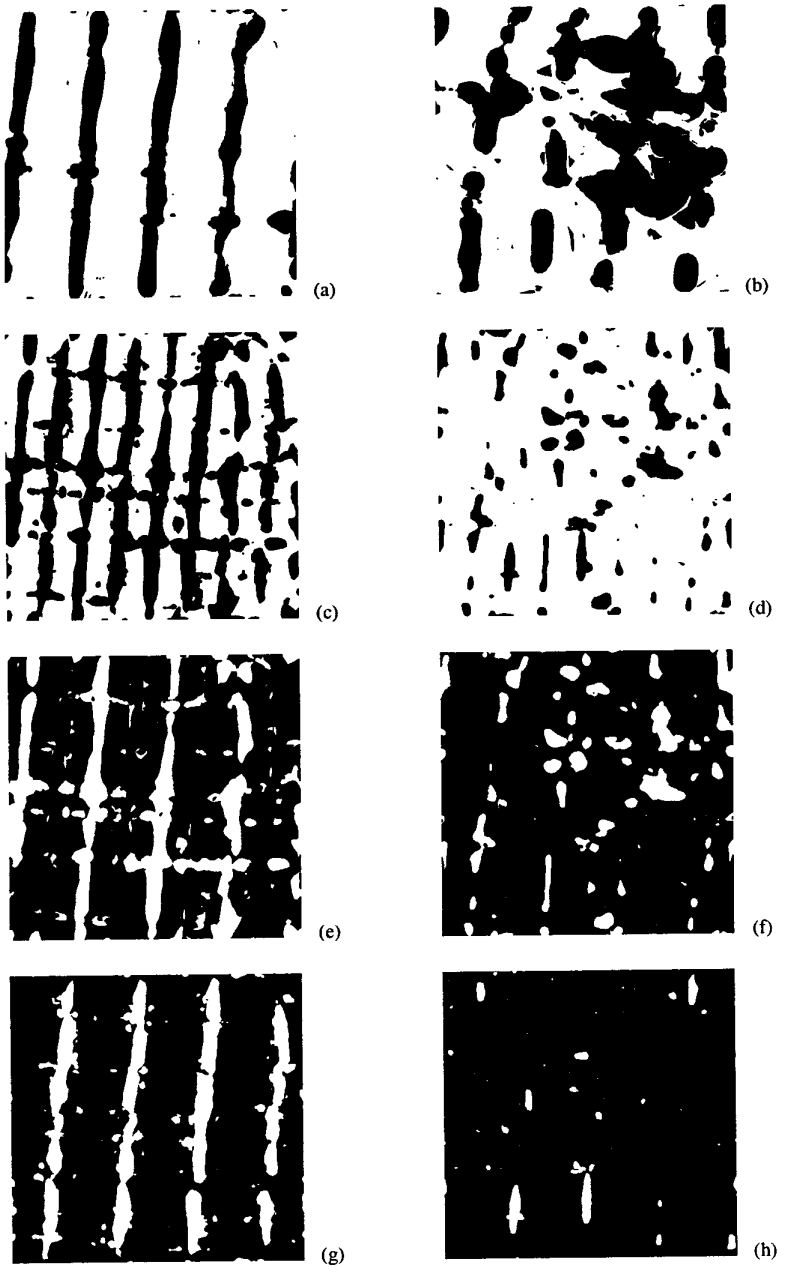

Figure 2: AM-FM analysis results II of II. In (a), (c), (e) and (g) we present results for the normal image, while in (b), (d), (f) and (h) we present results for the pathological image. For (a) and (b), we show the results for thresholding the amplitude: $a(\cdot) < 20$. The rest of the results are for the instantaneous frequency magnitude: $\| \nabla\phi \| < 0.046$ for (c) and (d), $0.046 < \| \nabla\phi \| < 0.08$ for (e) and (f), $0.08 < \| \nabla\phi \| < 0.15$ for (g) and (h).